Journal of Hydrology 519 (2014) 1953–1962

Contents lists available at ScienceDirect

Journal of Hydrology

journal homepage: www.elsevier.com/locate/jhydrol

Evolution of the hydro-climate system in the Lake Baikal basin

Rebecka Törnqvist, Jerker Jarsjö *, Jan Pietroń, Arvid Bring, Peter Rogberg, Shilpa M. Asokan, Georgia Destouni

Department of Physical Geography and Quaternary Geology, The Bolin Centre for Climate Research, Stockholm University, SE-106 91 Stockholm, Sweden

ARTICLE INFO

Article history:
Received 12 May 2014
Received in revised form 25 September 2014
Accepted 27 September 2014
Available online 7 October 2014
This manuscript was handled by Konstantine P. Georgakakos, Editor-in-Chief, with the assistance of Alon Rimmer, Associate Editor

Keywords:
Lake Baikal
Selenga River Basin
Climate change
CMIP5
Hydrology
Permafrost

SUMMARY

Climatic changes can profoundly alter hydrological conditions in river basins. Lake Baikal is the deepest and largest freshwater reservoir on Earth, and has a unique ecosystem with numerous endemic animal and plant species. We here identify long-term historical (1938–2009) and projected future hydro-climatic trends in the Selenga River Basin, which is the largest sub-basin (>60% inflow) of Lake Baikal. Our analysis is based on long-term river monitoring and historical hydro-climatic observation data, as well as ensemble mean and 22 individual model results of the Coupled Model Intercomparison Project, Phase 5 (CMIP5). Study of the latter considers a historical period (from 1961) and projections for 2010–2039 and 2070–2099. Observations show almost twice as fast warming as the global average during the period 1938–2009. Decreased intra-annual variability of river discharge over this period indicates basin-scale permafrost degradation. CMIP5 ensemble projections show further future warming, implying continued permafrost thaw. Modelling of runoff change, however, is highly uncertain, with many models (64%) and their ensemble mean failing to reproduce historical behaviour, and with indicated future increase being small relative to the large differences among individual model results.

1. Introduction

Global climate change can alter the terrestrial water cycle through changed magnitude, and spatial and temporal distribution of precipitation (defined as any form of water, such as rain or snow, that falls to the earth's surface; *P*), evaporation and evapotranspiration (defined as the sum of evaporation and transpiration from plants transferred from the earth's surface to the atmosphere; ET). For example, the frequencies of drought and flood may then change, and as temperatures change, the timing of melting and freezing events can change in response (Huntington, 2006; Asokan et al., 2010; Jarsjö et al., 2012; IPCC, 2013). In order to plan for sustainable water use that does not endanger society's water security or downstream ecosystems under changing climate conditions it is essential to assess both historical and future hydro-climatic changes (Varis et al., 2004; Destouni et al., 2013).

Generally, global warming has been observed to be particularly significant in the arctic and subarctic regions (Serreze et al., 2000), where thawing permafrost may also alter hydrologic conditions (Smith et al., 2007; Frampton et al., 2011; Karlsson et al., 2012). Hydro-climatic changes in these areas can also lead to ecosystem regime shifts related to, e.g., vegetation cover and thermokarst lake conditions (Karlsson et al., 2011; Poulter et al., 2013).

The drainage basin of the deepest and largest freshwater reservoir on Earth, Lake Baikal of southern Siberia (Russia), is situated in a subarctic climate zone (Brunello et al., 2006), and is almost entirely underlain of permafrost (Brown et al., 1997). Lake Baikal and its surroundings have been declared an UNESCO World Heritage Site due to their unique ecosystems with numerous endemic animal and plant species (UNESCO, 1996). Despite its large volume, the lake has already been impacted by the changing climate in terms of a prolonged ice-free season and higher water temperatures (Magnuson et al., 2000; Hampton et al., 2008). The overall warming of Lake Baikal has also had implications for its ecosystem (Hampton et al., 2008; Moore et al., 2009). Potential permafrost thaw in the lake's drainage basin may further change hydrological and ecosystem conditions, but the long-term hydro-climatic changes and their possible interactions with permafrost thaw have not been well investigated, even in the largest sub-basin, the Selenga River Basin.

In addition to climate-related changes, the Selenga River Basin is considered to be one of the most impacted areas with regard to heavy metal loads in the world (Thorslund et al., 2012). Mining is a major source of water contamination, and despite a rapidly developing economy of the region, relatively few measures have

* Corresponding author. Tel.: +46 8 16 49 58.
E-mail address: jerker.jarsjo@natgeo.su.se (J. Jarsjö).

http://dx.doi.org/10.1016/j.jhydrol.2014.09.074
0022-1694/

so far been taken to mitigate negative environmental impacts. Thus, significant amounts of heavy metals are released to the Selenga River system. They are prone to accumulate in and be transported with river sediment loads due to the basin's alkaline conditions (Brunello et al., 2006). The lower pH conditions in Lake Baikal imply that heavy metal transported in the metal-rich sediment loads can be dissolved in lake water (Chalov et al., 2014). Changed hydro-climatic conditions in the basin may lead to changes also in the loading patterns of industrial pollution and other substances, such as nutrients, into the Lake Baikal with additional change implications for its ecosystem (Moore et al., 2009). For instance, increased nutrient loading coupled with changed climatic conditions can cause profound impacts on large freshwater systems through algal bloom (Michalak et al., 2013).

Even though important, understanding and predicting impacts of global climate change on hydrological basins is scientifically challenging, due to issues of scale, spatio-temporal variability and process complexity (Bring and Destouni, 2011; Jarsjö et al., 2012; Teutschbein and Seibert, 2012; Trenberth and Asrar, 2012; Stevens and Bony, 2013). The Coupled Model Intercomparison Project, Phase 5 (CMIP5) allows for comparing and synthesising extensive hydro-climatic outputs from different Global Climate Models (GCMs), and has provided an essential basis for the compilation of the 5th IPCC report (Taylor et al., 2012; IPCC, 2013). Even though models have been developed from previous model generations, e.g., CMIP3 (Taylor et al., 2012), model uncertainties may still remain in individual and multi-model outputs of CMIP5 and may be particularly evident for hydro-climatic changes (Bring and Destouni, 2011, 2013, 2014).

In order to bridge current gaps in hydro-climatic change assessment for the major Selenga River Basin of Lake Baikal, we here investigate long-term historical and projected future conditions in this basin, with the main objectives to: (i) identify historical hydro-climatic trends and their possible causes, (ii) assess to which extent CMIP5 models can reproduce observed trends, and (iii) assess to which extent projected trends of CMIP5 models are consistent among different models and how they link to observed trends so far. We consider a historical period of 72-years (1938–2009) for which there are detailed discharge (Q) data. We expect changes in climate and in the landscape, such as permafrost thaw, to have relatively clear and detectable impacts on the system's hydrology and thereby on Q, as hydro-engineered structures that could distort these change impacts are generally absent in the basin. We furthermore assess and evaluate the performance of multi-model ensemble means and 22 individual model outputs of the CMIP5, considering their comparison with actual observation data and their projections for a near future period (2010–2039) and a more distant future period (2070–2099).

2. Method

2.1. Study site

Lake Baikal is the oldest (about 25 million years old) and deepest (1,637 m) freshwater lake in the world. It is inhabited by over 1500 endemic species and it stores about 20% of world's unfrozen fresh water (Brunello et al., 2006). Over 60% of the annual water inflow to Lake Baikal comes from its major tributary, the Selenga River. The river is about 943 km long and its basin area comprises about 80% of the total Lake Baikal drainage basin (Fig. 1). A large part of the Selenga River Basin has mountainous topography. Approximately 63% of the basin area of 477,000 km^2 is located in Mongolia, including the upstream part of the basin, which is dominated by an extensive grassland steppe. The downstream part is located in Southern Siberia, Russia (Mun et al., 2008) and is mainly covered by forest. The Selenga River Delta at the Lake Baikal outlet is the world's largest continental delta estuary (Logachev, 2003; Chalov et al., 2014).

The climate of the Selenga River Basin is extremely continental. The winters are long, dry and cold with average monthly surface air temperature (T) of January reaching −23.5 °C. Summers are short and relatively warm with monthly average T of July being 16.9 °C. There is a summer peak in P with about 50% of the P occurs in July and August (CRU TS3.10/CRU TS3.10.01 climate data; Harris et al., 2014). Due to harsh climate conditions the entire Selenga River Basin is underlined by mountain and arid-land permafrost. The permafrost extent varies from isolated patches in the central part of the basin (most of the Orkhon river basin and the downstream reach of the Selenga River), to continuous permafrost in the eastern and especially the western, mountainous parts of the basin (dark purple colours in Fig. 1; Brown et al., 1997). In most cases the permafrost temperature in the basin is close to 0 °C. Hence, the permafrost is thermally unstable and vulnerable to changing climate conditions and adverse human activities (Zhao et al., 2010).

2.2. Data and hydro-climatic assessment

We use area-averaged monthly data of T and P for the period 1938–2009 from the CRU TS3.10/CRU TS3.10.01 datasets (Harris et al., 2014). The area was determined from the extent of the Selenga River Basin, as delineated by estimating topography-controlled flow network based on digital elevation data (STRM; Farr et al., 2007). The CRU dataset is widely used and cited in large-scale climate investigations (Harris et al., 2014), and aims at a best-possible reproduction of the spatial pattern of T and P for each point in time, at 0.5 × 0.5 degree resolution. Although P may be highly variable on the scale of and within individual cells, and on short time periods, we consider the CRU dataset well suited to our application of estimating multi-annual changes over the relatively large region of the Selenga basin. We acknowledge, however, that values for some cells and some short periods may be more uncertain. This reasoning is supported by results from parallel research (Kamiguchi et al., 2010), which for instance has shown that when the number of P stations were greatly increased (from about 60 to 1300 over the area of Japan), it could have large influence on the representation of extreme events. However, the representation of longer time periods such as those considered in the present study was practically unaffected by the changed number of stations (Kamiguchi et al., 2010). For the Central Asian region, at least 80% of cells either have at least one station within the cell, or a station closer than the correlation decay distance (Harris et al., 2014: their Fig. 4). For the period 1950–1990, this figure is over 90%. More specifically, Fig. S1 of the Supplementary Information shows the locations of the approximately 40 T and P measurement stations that have been in use since at least the 1960s within and in the vicinity of the Selenga River Basin. The stations are spatially well distributed and cover an elevation range between 466 and 2117 meters, which practically the whole river basin is located within, with the exception of a few mountains in the relatively dry south-west part of the basin. These stations are hence likely to cover a near-full range of the different hydro-climatic conditions that exist within the basin.

Monitoring errors in P in mid and high latitude regions may be present due to undercatch of snow (Adam and Lettenmaier, 2003) and orographic effects due to underrepresentation of gauges at high elevations (Adam et al., 2006). Recognising the potential impact of these errors in the P dataset, we apply (i) a correction factor for undercatch and (ii) a combined correction factor for both undercatch and orographic effects on the P data. We evaluate the impact of these two alternative ways of data correction on presented results and conclusions. However, in order to keep

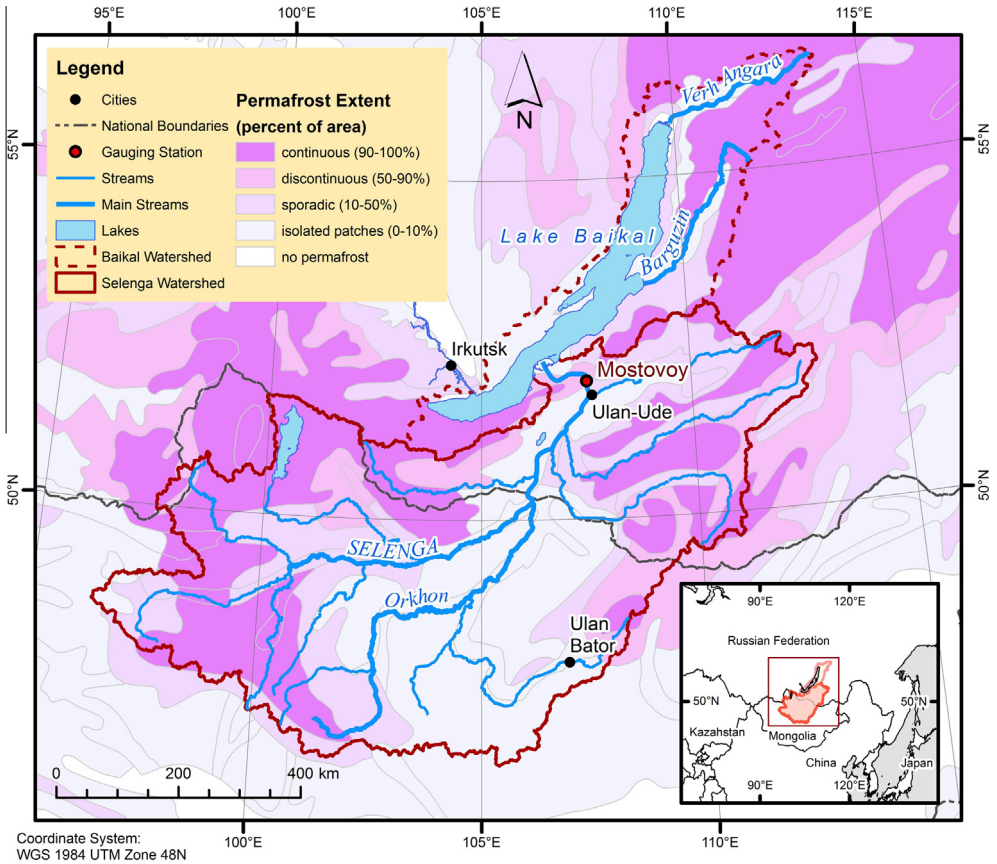

Fig. 1. The Lake Baikal drainage basin (dotted red line) and Selenga River Basin (solid red line) where purple colours indicate permafrost extent (Brown et al., 1997). Mostovoy gauging station is marked with a red dot. (For interpretation of the references to colour in this figure legend, the reader is referred to the web version of this article.)

biases related to overcorrection of measurement data as small as possible in the results presentation, we present full details only for the results of the method that gave the closest match between observation and CMIP5 multi-model ensemble mean.

Daily Q data for the gauging station Mostovoy (see Fig. 1 for location) for the period 1938–2009 was compiled from the Hydrometeorological Centre of Russia as part of a collaborative project (see Chalov et al., 2014). Analysis of intra-annual changes of Q with time was performed by considering daily Q over multiple years, and the minimum and maximum daily Q for each year. Average runoff (R) from the river basin (in mm/year) was calculated as average Q divided by the river basin area. The commonly used method of employing T as a proxy for ET has been shown to be less accurate than surface energy budget methods (Lofgren et al., 2013). However, surface energy budget methods require much more data input, which may not be available in sparsely populated river basins (Lofgren et al., 2013). In this study, we overcome this difficulty by estimating ET by closing the water balance, i.e., as $ET = P–R–\Delta S$, assuming the long-term average change in water storage (ΔS) to be close to zero. For T, P, ET, and R, long-term temporal patterns were analysed by calculating annual mean and seasonal mean values (defining winter as December, January and February, spring as March, April and May, summer as June, July and August, and autumn as September, October and November).

Although processes such as decay of permafrost may interfere with the assumption of long-term zero water balance, we expect the influence of these effects to be small. For instance, McClelland et al. (2004) concluded that attributing an observed increase in pan-Arctic discharge to thawing permafrost would require unreasonable volumes of melted ice. Furthermore, the principal effect of thawing permafrost on hydrology is most likely not through major changes in water balance over large regions, but instead on changed flow pathways and the timing of R (e.g., Frampton et al., 2011).

CMIP5 data were synthesized (Taylor et al., 2012). In particular, models with data on T, P, ET (termed evaporation in CMIP5 datasets) and R were selected and, since not all models provided multiple realizations, we chose to use only one member per model (to avoid model bias). The preferred choice was r1i1p1, where r is realization, i is initialization and p is perturbation. The NorESM1-M model was excluded due to errors in ET data. Table 1 lists all models used and affiliations responsible for the model development. Data for two future emission scenarios were selected (i) RCP2.6, a low emission scenario, and (ii) RCP8.5, a high emission scenario (see IPCC (2013) for details). For each model and emission scenario we computed area-weighted averages for T, P, ET and R. We also computed ensemble mean averages and standard deviations for the historical periods of 1961–1990, 1961–1980 and 1986–2005 as well as the future periods of 2010–2039 and 2070–2099.

To evaluate the performance of individual CMIP5 models, their output was ranked based on agreement with observed values for the period 1961–1990, as well as agreement with the magnitude of change between the periods 1961–1980 and 1986–2005. More specifically, a model was assigned rank 1 with respect to a specific parameter if its parameter value showed the lowest difference from the observed value among all models. Analogously, the model with the highest difference among the 22 models was assigned rank 22 (see e.g. Bring and Destouni, 2013). The ranking was performed for each parameter, and overall model ranks were assigned based on average rank for all parameters.

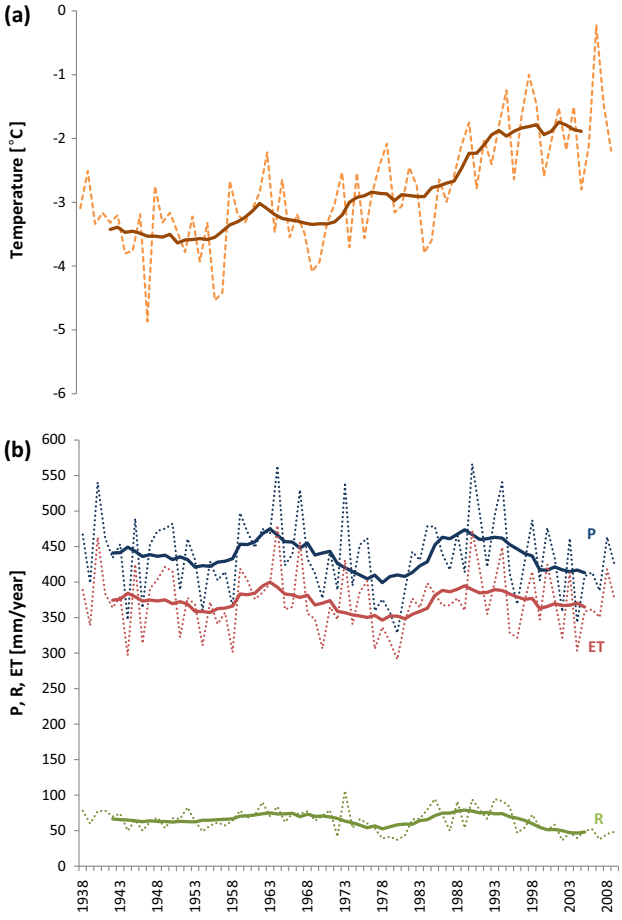

Fig. 2. Long-term patterns in mean annual (a) temperature (T), (b) precipitation (P), evapotranspiration (ET), and runoff (R) for the period 1938–2009 in the Selenga River Basin. Dashed lines indicate annual values and solid lines indicate 10-year running averages. Runoff is monitored at Mostovoy gauging station (see Fig. 1 for location).

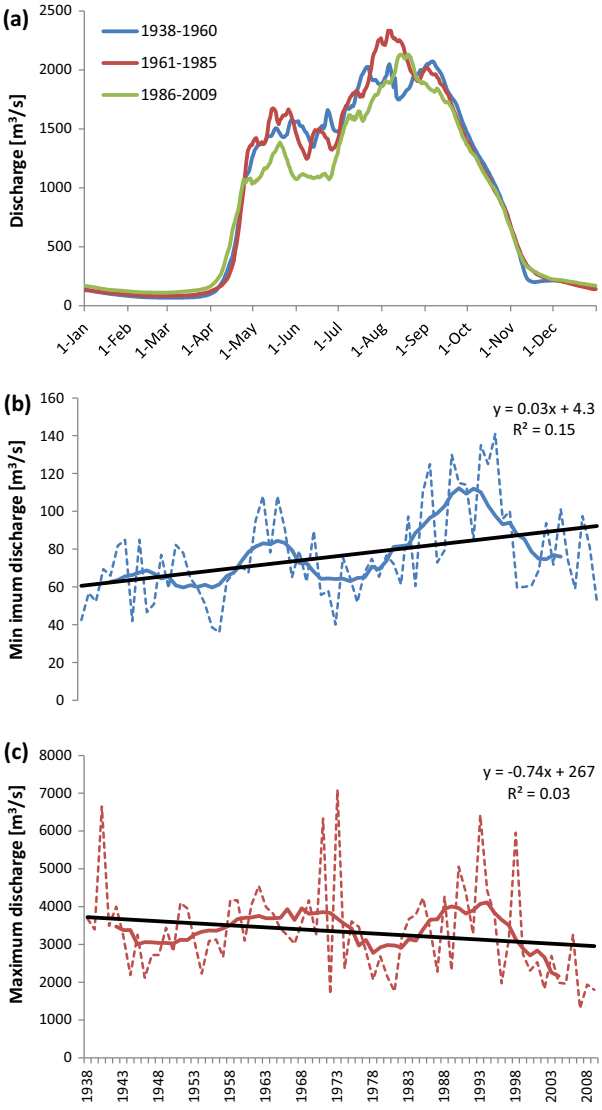

Fig. 3. (a) Changes in daily discharge (Q) pattern over the year for the periods 1938–1961, 1962–1985 and 1986–2009, and temporal pattern of (b) minimum and (c) maximum daily Q within a year for the period 1938–2009 at the Mostovoy gauging station (see Fig. 1 for location). Linear trend lines (in black solid lines), annual values (in blue and red dashed lines) and 10-year running averages (in blue and red solid lines) are shown. (For interpretation of the references to colour in this figure legend, the reader is referred to the web version of this article.)

3. Results

3.1. Observed hydro-climatic changes

There has been an observed increase in mean annual T in the Selenga River Basin by 1.6 °C or 0.022 °C/year during the considered historical period 1938–2009 (based on 10-year running averages; Fig. 2a). This is almost twice as much as the global average warming rate of 0.012 °C/year (0.72 °C increase during the period 1951–2012; IPCC, 2013). The difference in considered periods in this study (1938–2009) and in IPCC (2013; 1951–2009) should be noted. Moreover, the warming rate of the Selenga River Basin was about two times higher during the latest 20-year period (1989–2009; 0.048 °C/year) than during the whole 72-year period (0.022 °C/year; Fig. 2a), which is in agreement with the global pattern of increased warming rates during this period (IPCC, 2013). Furthermore, the periods during which T is above the water freezing point have become longer in recent years. For instance, the 10-year running average T of April has been above 0 °C since 1992.

Uncorrected CRU-data on average P of the historical 1961–1990 period was on average 26% lower than the corresponding CMIP5 ensemble mean P. Correction of P for undercatch resulted in a corrected P that was 15% lower than the modelled CMIP5 ensemble mean (Fig. S2 in Supplementary Information). However, correction of P for both undercatch and orographic effects resulted in a corrected P that was 18% higher than the modelled CMIP5 ensemble mean (Fig. S2). In the following sections, presented detailed results are based on P-data corrected for undercatch only, in order to keep biases related to overcorrection of data as small as possible. We note however that our conclusions are robust with regard to choice of P-correction method.

The annual mean values of the water balance components P, ET and R, exhibit relatively small temporal changes during the historical period (Fig. 2b). For instance, although there is some variation, there is no consistent trend in R on longer (multi-decadal) timescales. However, R has slightly decreased since 1990. The 10-year running average reaches its minimum value at the end of the investigation period (Fig. 2b). Comparing the two 20-year periods of 1961–1980 and 1986–2005, the annual mean P and ET both increased with 7.8 and 9.1 mm, respectively, resulting in an insignificant R decrease of 1.3 mm. Considering absolute values, the largest part of P (85%) is lost through ET. This is in agreement with an independent estimate of the ET/P ratio being 81% in the Mongolian part of the basin for the period 1988–1992, where ET was estimated with the Penman–Montieth method (Ma et al., 2003).

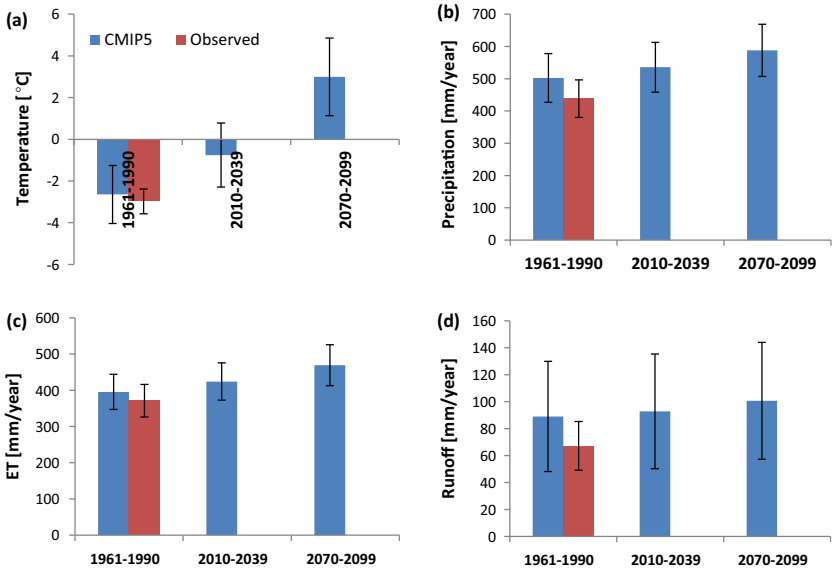

Fig. 4. Observed mean values for the period 1961–1990 (in red) and CMIP5 ensemble means for the periods 1961–1990, 2010–2039 and 2070–2099 (in blue) for (a) temperature (*T*), (b) precipitation (*P*), (c) evapotranspiration (ET) and (d) runoff (*R*). The future projections are under the high emission scenario RCP8.5. Error bars around blue bars indicate standard deviation around the multi-model ensemble mean. Error bars around red bars indicate standard deviation of annual fluctuations. (For interpretation of the references to colour in this figure legend, the reader is referred to the web version of this article.)

Table 1
CMIP5 models used in the hydro-climatic assessment.

No.	Model name	Institute
1	BNU-ESM	College of Global Change and Earth System Science, Beijing Normal University
2	CCSM4	National Center for Atmospheric Research
3	CNRM-CM5	Centre National de Recherches Météorologiques/Centre Européen de Recherche et Formation Avancée en Calcul Scientifique
4	CSIRO-Mk3-6-0	Commonwealth Scientific and Industrial Research Organization in collaboration with Queensland Climate Change Centre of Excellence
5	CanESM2	Canadian Centre for Climate Modelling and Analysis
6	FGOALS-g2	LASG, Institute of Atmospheric Physics, Chinese Academy of Sciences and CESS, Tsinghua University
7	FIO-ESM	The First Institute of Oceanography, SOA, China
8	GFDL-CM3	NOAA Geophysical Fluid Dynamics Laboratory
9	GFDL-ESM2G	NOAA Geophysical Fluid Dynamics Laboratory
10	GISS-E2-H	NASA Goddard Institute for Space Studies
11	GISS-E2-R	NASA Goddard Institute for Space Studies
12	IPSL-CM5A-LR	Institut Pierre-Simon Laplace
13	IPSL-CM5A-MR	Institut Pierre-Simon Laplace
14	MIROC-ESM	Japan Agency for Marine-Earth Science and Technology, Atmosphere and Ocean Research Institute (The University of Tokyo), and National Institute for Environmental Studies
15	MIROC-ESM-CHEM	Japan Agency for Marine-Earth Science and Technology, Atmosphere and Ocean Research Institute (The University of Tokyo), and National Institute for Environmental Studies
16	MIROC5	Atmosphere and Ocean Research Institute (The University of Tokyo), National Institute for Environmental Studies, and Japan Agency for Marine-Earth Science and Technology
17	MPI-ESM-LR	Max-Planck-Institut für Meteorologie (Max Planck Institute for Meteorology)
18	MPI-ESM-MR	Max-Planck-Institut für Meteorologie (Max Planck Institute for Meteorology)
19	MRI-CGCM3	Meteorological Research Institute
20	NorESM1-ME	Norwegian Climate Centre
21	Bcc-csm1-1	Beijing Climate Center, China Meteorological Administration
22	Bcc-csm1-1-m	Beijing Climate Center, China Meteorological Administration

The absence of long-term *R* trends is consistent with fragmented and potentially opposing land-use trends in the basin. For instance, in the Mongolian upper parts of the basin, the arable land showed a general decrease between the early 1990s and around 2005 (Priess et al., 2011). After that, the arable land has expanded and the proportion of irrigated fields has also increased. However, even in the parts of Mongolia that have the most intense agriculture, the arable land covers only a very small proportion (around 4%; FAO, 2014) of the Mongolian part of the basin and is therefore likely to have a minor influence on *R* generation, in particular since irrigation is not well developed in absolute terms. In the Russian part of the basin, the area of arable land has decreased since the 1980s, however also in this case the irrigation water use is relatively low and the change concerns a relatively small part (3%; Bazhenova and Kobylkin, 2013) of the forest-dominated basin. In contrast, forestry is increasing in the Russian part of the basin (Bazhenova and Kobylkin, 2013). Overall, whereas there are no obvious correlations between land use change and observed *R* variation Fig. 2b indicates that the period of slightly higher *R* around the 1990s coincides with a period of higher *P*.

The observed average annual Q of the Selenga River at Mostovoy gauging station is about 855 m^3/s for the period 1938–2009. During the cold period, between November and March, most rivers in the basin are frozen and observed Q is small, around 80–100 m^3/s. The largest Q in the Selenga River is observed in August, when it reaches over 2000 m^3/s (Fig. 3a). The observed decrease of Q in

recent years is largely due to decreased peak discharges during summer (Fig. 3a). However, the winter base flow has increased. Therefore, there is an overall temporal increase in minimum annual Q and a decrease in maximum annual Q (no significant linear regression coefficients; Fig. 3b and c), resulting in a decreased intra-annual variability. Results of detailed process-based numerical simulations have indicated such decrease as an expected hydrological change impact of permafrost thaw in a warming climate (Frampton et al., 2011).

More generally, observations show that the changes in the main hydro-climatic parameters differ between winter, spring, summer and autumn, as here exemplified for average seasonal changes in T, P, R and P–R (reflecting change in ET and/or in storage) between the periods 1961–1985 and 1986–2009 (Fig. S3 of Supplementary Information). The largest and smallest seasonal T increases occurred in winter (1.32 °C) and autumn (0.85 °C), respectively. The largest P increase has occurred in spring, whereas summers and winters show only small increases in P (on the order of 1 mm). By contrast, P has decreased in autumn. Furthermore, R (derived from observed Q; Fig. 3a) has decreased during all seasons except winter. The largest decrease in R is shown during summer. Taken together, increased P and decreased R during spring and summer implies largely increased P–R during those seasons, which must be due to increased ET or increased water storage, for instance in groundwater, or a combination of both. By contrast, in autumn the decrease in P is much larger than the decrease in R, which implies decreased ET and/or storage.

3.2. CMIP5 model output versus historical observations

Fig. 4 shows observed historic mean values of the Selenga River Basin's T, P, ET and R (red bars; left hand side) compared to the CMIP5 multi-model ensemble mean of historical (left hand side; blue bars) and future (right hand side) projections under a high emission scenario. For the historical period 1961–1990, the CMIP5 ensemble mean overestimates the observed mean T with 0.3 °C, the undercatch corrected P with 15%, ET with 6% and R with 24% (left hand side in Fig. 4a–d). The ensemble mean, and the majority of the 22 models overestimate the observed T (14 models), P (18 models), ET (15 models) and R (15 models; Table 2; Fig. S4 in Supplementary Information). With regard to change, Fig. 5 shows that the ensemble mean of modelled change in P (ΔP) is greater than the observed change, while the modelled ΔET is smaller than the observed from water balance closure. This yields a modelled increase in the ensemble mean R between the two periods (positive ΔR) in contrast to the observed slight decrease in R (negative ΔR, Fig. 5). Only eight models of 22 reproduced the observed slightly negative ΔR (with an overestimation of the negative ΔR; Table 2).

Table 3 shows our model ranking of how close CMIP5 predictions are to observed absolute values considering the period 1961–1990, and how close CMIP5 predictions are to observed change considering differences between 1961–1980 and 1986–2005. The best overall model performance (all parameters considered), with smallest average difference in absolute parameter values, was shown by bcc-csm1-1 (model number 21). In reproducing observed change, MPI-ESM-LR (model number 17) performed best. However, another model (GISS-E2-R, model number 19) performed best in reproducing the observed R, and yet another (MRI-CGCM3, model number 11) performed best in reproducing the observed ΔR (Table 3); the latter model; however, yielded wrong directions for both ΔP and ΔET (Fig. 5).

Furthermore, the two best ranked models with regard to absolute parameter values (model number 21 and 19; Table 3) failed to reproduce the observed direction of change in R (i.e., the negative ΔR; this is also true for the above mentioned model number 17). Model number 21 yields also opposite direction of ΔET than observed, whereas model number 19 yields opposite direction of ΔP (Fig. 5b). Overall, Fig. 5 shows the difficulty of the CMIP5 model ensemble to accurately reproduce, both absolute values and changes of each and across all hydrological variables, even for the best performing models.

3.3. Projection of future changes

Under a high emission scenario (RCP8.5; Fig. 4), the mean annual T of −2.5 °C for the period 1961–1990 could increase to as much as 3 °C for 2070–2099 (Fig. 4a). Such a shift from negative to positive mean annual T should be expected to yield further permafrost thaw in the future. The magnitudes of P, ET and R are expected to increase in the future (Fig. 4b–d). However, especially the projected future R is uncertain due to its small projected increase relative to the large differences among individual model results, as shown by the large standard deviation (error bars) in Fig. 4d.

The future scenarios of low emissions (RCP2.6) and high emissions (RCP8.5) yield similar projections of T, P, ET and R for the period 2010–2039 (Fig. S5 in Supplementary Information). For instance, the two scenarios are projected to yield T increases of between 1.6 and 1.9 °C and P increase of 6.5%. The discrepancy between the low and high emission scenarios increases for the more distant future period of 2070–2099, for which the projected values of ΔT, ΔP, ΔET and ΔR for the high emission scenario are more than twice those for the low emission scenario (Fig. S5).

4. Discussion

4.1. Observed hydro-climatic changes

The considerable T change (warming) of 0.022 °C/year for the Selenga River Basin (1938–2009) is almost twice as high as the global mean warming, but in the same range as the warming of other regions in Central Asia. For instance, the Aral Sea Drainage Basin has a warming rate of 0.015 °C/year (for the period 1901–2002;

Table 2
Assessment of individual CMIP5 models ability to model observed mean absolute values for the 1961–1990 period in terms of number of models: (1) which overestimate observations, and (2) underestimate observations, and changes between the 1961–1980 and 1986–2005 periods in terms of number of models (3) which model the observed direction of change but overestimate observations, (4) which model the observed direction of change but underestimate observations, and (5) which model different direction of trend than observed for temperature (T), precipitation (P), evapotranspiration (ET) and runoff (R).

	T	P	ET	R
Absolute values 1961–1990				
(1) No. models which overestimate observations	14 (64%)	18 (82%)	15 (68%)	15 (68%)
(2) No. models which underestimate observations	8 (36%)	4 (18%)	7 (32%)	7 (32%)
Change between 1961–1980 and 1986–2005				
(3) No. models which overestimate observations, with same direction as the observed change	4 (18%)	11 (50%)	10 (45%)	8 (36%)
(4) No. models which underestimate observations, with same direction as the observed change	18 (82%)	4 (18%)	5 (23%)	0 (0%)
(5) Different direction of change than observed	0 (0%)	7 (32%)	7 (32%)	14 (64%)

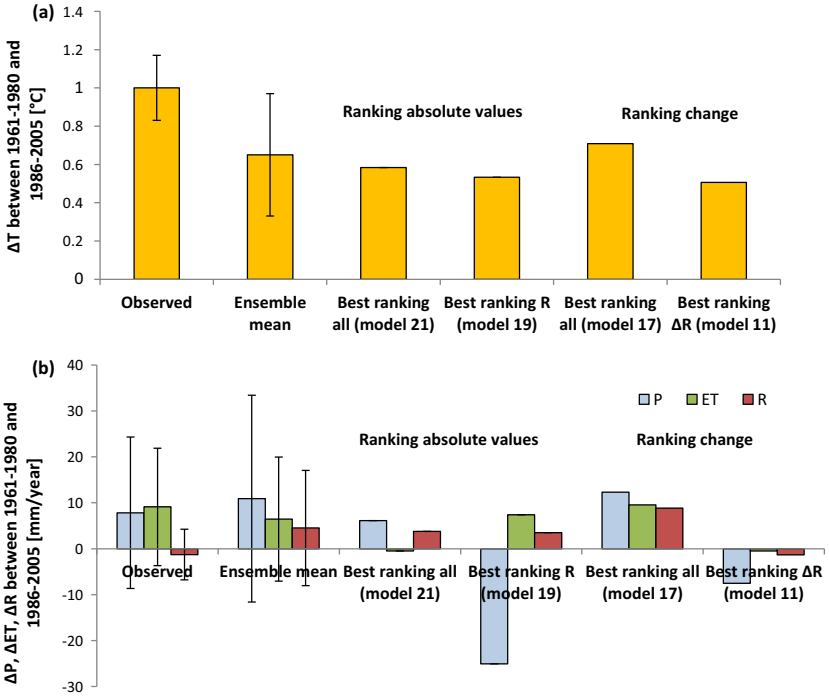

Fig. 5. Observed and modelled (a) temperature change (ΔT) and (b) precipitation change (ΔP), evapotranspiration change (ΔET) and runoff change (ΔR) between 1961–1980 and 1986–2005. CMIP5 multi-model ensemble means and best ranked models for (i) modelling absolute values for the period 1961–1990 based on average best rank for all parameters (model nr 21 bcc-csm1-1) and for R (model nr 19 MRI-CGCM3) and (ii) modelling change between 1961–1980 and 1986–2005 based on average best rank for all parameters (model nr 17 MPI-ESM-LR) and for ΔR (model nr 11 GISS-E2-R), are shown. Error bars indicate: (i) 80% confidence intervals for the observed annual change between the periods (see details on calculations in Asokan and Destouni, 2014) and (ii) standard deviation around the multi-model ensemble mean.

Table 3
Ranking of the considered CMIP5 models regarding their ability of modelling the observed temperature (T), precipitation (P), evapotranspiration (ET), runoff (R) and average and overall rank considering all four parameters, based on (i) mean values for the period 1961–1990 and (ii) change between 1961–1980 and 1986–2005. Best ranked model for each category is marked in bold.

Model		Rank of modelling absolute values						Rank of modelling change					
		T	P	ET	R	Average	Overall rank	ΔT	ΔP	ΔET	ΔR	Average	Overall rank
1	BNU-ESM	**1**	22	18	9	12.5	11	12	18	18	20	17.0	16
2	CCSM4	7	14	16	4	10.3	7	7	16	9	17	12.3	11
3	CNRM-CM5	19	9	**1**	16	11.3	8	8	7	11	2	7.0	2
4	CSIRO-Mk3-6-0	10	8	22	5	11.3	8	13	2	22	16	13.3	14
5	CanESM2	14	11	19	8	13.0	12	2	9	17	6	8.5	4
6	FGOALS-g2	22	2	3	13	10.0	6	5	10	10	9	8.5	4
7	FIO-ESM	15	21	2	22	15.0	14	9	12	2	18	10.3	7
8	GFDL-CM3	6	10	17	3	9.0	5	19	3	3	4	7.3	3
9	GFDL-ESM2G	5	3	14	11	8.3	4	**1**	20	21	5	11.8	10
10	GISS-E2-H	20	5	15	17	14.3	14	21	8	14	3	11.5	9
11	GISS-E2-R	18	**1**	13	15	11.8	10	17	14	15	**1**	11.8	10
12	IPSL-CM5A-LR	17	18	4	21	15.0	14	3	17	13	19	13.0	13
13	IPSL-CM5A-MR	8	16	6	20	12.5	11	4	21	6	22	13.3	14
14	MIROC-ESM	13	20	21	19	18.3	16	15	5	7	14	10.3	7
15	MIROC-ESM-CHEM	11	19	20	18	17.0	15	11	13	4	12	10.0	6
16	MIROC5	21	4	9	7	10.3	7	10	11	19	10	12.5	12
17	MPI-ESM-LR	12	17	12	14	13.8	13	6	4	**1**	15	**6.5**	**1**
18	MPI-ESM-MR	16	13	8	10	11.8	10	20	22	20	21	20.8	17
19	MRI-CGCM3	3	7	11	**1**	5.5	2	16	19	5	7	11.8	10
20	NorESM1-ME	9	15	10	12	11.5	9	22	15	16	11	16.0	15
21	Bcc-csm1-1	2	6	5	2	**3.8**	**1**	14	**1**	12	8	8.8	5
22	Bcc-csm1-1-m	4	12	7	6	7.3	3	18	6	8	13	11.3	8

Jarsjö et al., 2012) and the Predbaikalie area north of Lake Baikal has a warming rate of 0.039 °C/year (for the period 1960–2000; Voropay et al., 2011). The increased T in the Selenga River Basin implies that the surface thaw index has increased (cumulative degree-days per year over 0 °C; Wu et al., 2011). Furthermore, relatively sparse point data from monitoring of boreholes in the Mongolian part of the Selenga River Basin show permafrost temperature increase of 0.01–0.03 °C/year, and increase of active layer extent of 0.1–0.6 cm/year (Sharkhuu, 2003; Zhao et al., 2010).

The present Q analysis of the downstream Selenga River shows a decreased intra-annual variability of Q, with decreased peak flow and increased base flow. This has been indicated by simulations as a clear hydrological change impact of permafrost thaw (Frampton et al., 2011) and has been found also in basin-scale studies of

permafrost thaw impacts on hydrology (Karlsson et al., 2012). This study thus supports regional point observations of permafrost degradation by Sharkhuu (2003) and Zhao et al. (2010) and suggests that such changes may prevail across the whole basin. Such a basin-scale degradation of permafrost could change transport pathways of water and waterborne pollutants (Bosson et al., 2013) in addition to increasing the active layer depth and groundwater contributions to stream flow (Smith et al., 2007).

Our results further show a slight decrease of observed mean annual Q since 1990, which is largely due to decreased peak discharge during summer (Fig. 3). Such decreased Q peaks and average Q may have large influence on sediment transport. In consistency, monitored long-term sediment transport patterns in the lower Selenga River (Mostovoy gauging station) indicate progressing decrease of sediment loads since the 1970s (Chalov et al., 2014). Since the sediments in many cases contain relatively high metal concentrations from, e.g., mining operations (Thorslund et al., 2012), shifts in sediment transport patterns from altered hydrology within the Selenga River Basin may also influence the heavy metal loading to Lake Baikal. Above-discussed historical trends hence suggest lower loads of metals in recent years, all other conditions equal.

4.2. CMIP5 model output versus historical observations

For the period 1961–1990, the CMIP5 multi-model ensemble mean overestimates all hydro-climatic variables: T with 11%, P with 13%, ET with 6% and R with 24%. In contrast, in the largest basin in Central Asia, the Aral Sea Drainage Basin, the modelled R is overestimated as much as 600%, which is largely because most GCMs neglect the ET-increasing and thereby R-decreasing effects of intense irrigation (Destouni et al., 2010; Törnqvist and Jarsjö, 2012; Jarsjö et al., 2012; Asokan and Destouni, 2014). In the Selenga River Basin, hydrological effects of water use including intensified agriculture are much less pronounced, and conditions are therefore closer to natural ones, as assumed by the GCMs.

Most CMIP5 models and their ensemble mean failed to reproduce the historical decrease in R of the Selenga River Basin between the two 20-year periods 1961–1980 and 1986–2005. This raises the question of whether or not results could be improved by extending or refining the CMIP5 models' process descriptions, in analogy with the more obvious example of accounting for irrigation effects on ET and R in the Aral Sea drainage basin. For instance, the CMIP5 models do not include all processes needed to capture permafrost change and its impact on hydrology (IPCC, 2013). Analyses of Slater and Lawrence (2013) and Koven et al. (2013) showed large discrepancies between CMIP5 models in simulating the current permafrost extent and its historical changes. The accuracy of land surface models was thus identified as a key limitation. In addition to the above-discussed decrease in intra-annual Q variability, the observed slight decrease in average Q and R even though P has increased in the Selenga River Basin may also be indicative of increased groundwater recharge associated with permafrost thaw (Hinzman et al., 2005; Smith et al., 2007; Bosson et al., 2012).

4.3. Projection of future changes

Future climate projections by the CMIP5 models under the RCP8.5 high-emission scenario converge on indicating large increase in T, by as much as 5 °C until the end of the century (2070–2099; Fig. 4a). Continued permafrost thawing in the Selenga River Basin is hence likely throughout the century. Globally, by the end of the 21st century, the permafrost extent is projected to decrease by 80%, and discontinuous permafrost is expected to vanish completely due to increased T under the RCP8.5 scenario (Slater and Lawrence, 2013).

In contrast to the T results, a large spread in ensemble results of the CMIP5 models shows considerable uncertainty in projections of future changes in all water balance components (ΔP, ΔET and ΔR), and particularly high uncertainty for ΔR. Even though most individual models as well as the CMIP5 ensemble mean result indicate an increased R in the future, this R increase is much smaller than the spread in individual model results. If it actually occurs; however, such a future R increase may, for instance, imply increased transport of (contaminated) sediments through the river systems of the Selenga basin to Lake Baikal (e.g., Chalov et al., 2014).

The highly uncertain projections of increased R in the future may be a result of model-related artefacts that influence model results for both the past and the future. More generally, there are many examples for different world regions of the difficulty of global models to accurately model water changes in the landscape (e.g., Bring and Destouni, 2011, 2013, 2014; Jarsjö et al., 2012; Fry et al., 2014). There is therefore a need for more accurate consideration of landscape-internal drivers and effects of hydrological change, such as permafrost thaw and/or changes in land use and water use, either in special hydrological modules of GCMs or in external hydrological models connected to GCMs.

5. Conclusions

- In the major Selenga River Basin within the Lake Baikal drainage basin, T has increased by almost twice the global average warming rate during the historical period 1938–2009.
- An observed decreased intra-annual variability of Q, evident in decreased peak flow and increased base flow during the period 1938–2009, is indicative of basin-scale permafrost thaw.
- CMIP 5 ensemble projections imply continued T increase, by as much as 5 °C until the end of the century (2070–2099). Permafrost thaw in the Selenga River Basin is hence also likely to continue throughout the century.
- Observed changes in the mean annual water balance components P, ET and R between 1961–1980 and 1986–2005 were relatively small. However, R has decreased since 1990, which is consistent with independent observations of decreased riverine sediment loads.
- However, half or more of the CMIP5 models and the multi-model ensemble mean overestimate the historical increase of P and underestimate or fail to yield an increase of ET (Table 2). As a consequence, a majority (64%, Table 2) of the models and their ensemble mean fail to reproduce the historical R change behaviour in the Selenga River Basin.
- Not even the overall best performing individual models could accurately reproduce observed water balance changes, and the multi-model ensemble mean should be preferred over individual model selection in assessment of future hydrological trends.
- Most individual models as well as the CMIP5 ensemble mean result indicate increased R in the future, but this is subject to particularly high uncertainty as the indicated future R increase is small and there are large differences among individual model projections. Since many CMIP5 models fail to reproduce the historical R change behaviour, projections of increased R in the future may be a result of model-related artefacts.
- In general, there is a large spread in the CMIP5 ensemble results regarding future changes of all water balance components (ΔP, ΔET and particularly so for ΔR), indicating considerable uncertainty in change projections for water in the landscape. This implies that large-scale climate and GCMs need to more accurately account for hydrological effects of landscape-internal changes in ambient conditions, such as thawing permafrost and changes in land use and water use.

Acknowledgement

The work was funded through the Swedish Research Council Formas (Project 2012-790).

Appendix A. Supplementary material

Supplementary data associated with this article can be found, in the online version, at http://dx.doi.org/10.1016/j.jhydrol.2014.09.074.

References

Adam, J.C., Lettenmaier, D.P., 2003. Adjustment of global gridded precipitation for systematic bias. J. Geophys. Res. 108, 1–14.
Adam, J.C., Clark, E.A., Lettenmaier, D.P., Wood, E.F., 2006. Correction of global precipitation products for orographic effects. J. Clim. 19, 15–38.
Asokan, S.M., Destouni, G., 2014. Irrigation effects on hydro-climatic change: basin-wise water balance-constrained quantification and cross-regional comparison. Surv. Geophys. 35, 879–895. http://dx.doi.org/10.1007/s10712-013-9223-5.
Asokan, S.M., Jarsjö, J., Destouni, G., 2010. Vapor flux by evapotranspiration: effects of changes in climate, land use, and water use. J. Geophys. Res. Atmos. 115, D24102.
Bazhenova, O.I., Kobylkin, D.V., 2013. The dynamics of soil degradation processes within the Selenga basin at the agricultural period. Geogr. Nat. Resour. 34 (3), 221–227.
Bosson, E., Sabel, U., Gustafsson, L.G., Sassner, M., Destouni, G., 2012. Influences of shifts in climate, landscape, and permafrost on terrestrial hydrology. J. Geophys. Res.-Atmos. 117, D05120.
Bosson, E., Selroos, J.-O., Stigsson, M., Gustafsson, L.-G., Destouni, G., 2013. Exchange and pathways of deep and shallow groundwater in different climate and permafrost conditions using the Forsmark site, Sweden as an example catchment. Hydrogeol. J. 21, 225–237.
Bring, A., Destouni, G., 2011. Relevance of hydro-climatic change projection and monitoring for assessment of water cycle changes in the Arctic. Ambio 40, 361–369.
Bring, A., Destouni, G., 2013. Hydro-climatic changes and their monitoring in the Arctic: observation-model comparisons and prioritization options for monitoring development. J. Hydrol. 492, 273–280.
Bring, A., Destouni, G., 2014. Arctic climate and water change: model and observation relevance for assessment and adaptation. Surv. Geophys. 35, 853–877. http://dx.doi.org/10.1007/s10712-013-9267-6.
Brown, J., Ferriansm, O.J., Heginbottom, J.A., Melnikov, E.S., 1997. Circum-Arctic Map of Permafrost and Ground Ice Conditions. USGS, Map CP-45, Scale 1:10,000,000. Natl. Snow and Ice Data Cent., World Data Cent. for Glaciol., Boulder, Colo.
Brunello, A.J., Molotov, V.C., Dugherkuu, B., Goldman, C., Khagamanova, E., Strijhova, T., Sigman, R., 2006. Lake Baikal. Experience and Lessons Learned. Brief. Tahoe-Baikal Institute, South Lake Tahoe.
Chalov, S.R., Jarsjö, J., Kasimov, N.S., Romanchenko, A., Pietroń, J., Thorslund, J., Belazerova, E., 2014. Spatio-temporal variation of suspended transport in the Selenga Basin (Mongolia and Russia). Environ. Earth Sci. http://dx.doi.org/10.1007/s12665-014-3106-z.
Destouni, G., Asokan, S.M., Jarsjö, J., 2010. Inland hydro-climatic interaction: effects of human water use on regional climate. Geophys. Res. Lett. 37 (18), L18402. http://dx.doi.org/10.1029/2010GL044153.
Destouni, G., Jaramillo, F., Prieto, C., 2013. Hydroclimatic shifts driven by human water use for food and energy production. Nat. Clim. Change 3, 213–217.
FAO, 2014. AQUASTAT – FAO's global water information system, <http://www.fao.org/nr/water/aquastat/countries_regions/MNG/index.stm> (accessed 18.08.2014).
Farr, T.G., Rosen, P.A., Caro, E., Crippen, R., Duren, R., Hensley, S., Kobrick, M., Paller, M., Rodriguez, E., Roth, L., Seal, D., Shaffer, S., Shimada, J., Umland, J., Werner, M., Oskin, M., Burbank, D., Alsdorf, D.E., 2007. The shuttle radar topography mission. Rev. Geophys. 45. http://dx.doi.org/10.1029/2005RG000183, RG2004.
Frampton, A., Painter, S., Lyon, S.W., Destouni, G., 2011. Non-isothermal, three-phase simulations of near-surface flows in a model permafrost system under seasonal variability and climate change. J. Hydrol. 403, 352–359.
Fry, L.M. et al., 2014. The Great Lakes Runoff Intercomparison Project Phase 1: Lake Michigan (GRIP-M). J. Hydrol. http://dx.doi.org/10.1016/j.jhydrol.2014.07.021.
Hampton, S.E., Izmest'eva, L.R., Moore, M.V., et al., 2008. Sixty years of environmental change in the world's largest freshwater lake – Lake Baikal, Siberia. Glob. Change Biol. 14, 1947–1958. http://dx.doi.org/10.1111/j.1365-2486.2008.01616.x.
Harris, I., Jones, P.D., Osborn, T.J., Lister, D.H., 2014. Updated high-resolution grids of monthly climatic observations – the CRU TS3.10 Dataset. Int. J. Clim. 34, 623–642. http://dx.doi.org/10.1002/joc.3711.
Hinzman, L.D., Bettez, F.S., Chapin, M.B., et al., 2005. Evidence and implications of recent climatic change in northern Alaska and other arctic regions. Clim. Change 72, 251–298.
Huntington, T.G., 2006. Evidence for intensification of the global water cycle: review and synthesis. J. Hydrol. 319, 83–95. http://dx.doi.org/10.1016/j.jhydrol.2005.07.003.
Intergovernmental Panel on Climate Change (IPCC), 2013. In: Stocker, T.F., Qin, D., Plattner, G.K., Tignor, M., Allen, S.K., Boschung, Y, Nauels, A., Xia, Y., Bex, V., Midgley, P.M. (Eds.), Climate Change 2013: The Physical Science Basis. Contribution of Working Group I to the Fifth Assessment Report of the Intergovernmental Panel on Climate Change. Cambridge University Press, Cambridge, United Kingdom and New York, NY, USA, 1535pp.
Jarsjö, J., Asokan, S.M., Prieto, C., Bring, A., Destouni, G., 2012. Hydrological responses to climate change conditioned by historic alterations of land-use and water-use. Hydrol. Earth Syst. Sci. 16, 1335–1347.
Kamiguchi, K., Arakawa, O., Kitoh, A., Yatagai, A., Hamada, A., Yasutomi, N., 2010. Development of APHRO_JP, the first Japanese high-resolution daily precipitation product for more than 100 years. Hydrol. Res. Lett. 4, 60–64.
Karlsson, J.M., Bring, A., Peterson, G.D., Gordon, L.J., Destouni, G., 2011. Opportunities and limitations to detect climate-related regime shifts in inland Arctic ecosystems through eco-hydrological monitoring. Environ. Res. Lett. 6, 014015. http://dx.doi.org/10.1088/1748-9326/6/1/014015.
Karlsson, J.M., Lyon, S.W., Destouni, G., 2012. Thermokarst lake, hydrological flow and water balance indicators of permafrost change in Western Siberia. J. Hydrol. 464–465, 459–466.
Koven, C.D., Riley, W.J., Stern, A., 2013. Analysis of permafrost thermal dynamics and response to climate change in the CMIP5 earth system models. J. Clim. 26 (6), 1877–1900. http://dx.doi.org/10.1175/JCLI-D-12-00228.1.
Lofgren, B.M., Gronewold, A.D., Acciaioli, A., Cherry, J., Steiner, A.L., Watkins, D.W., 2013. Methodological approaches to projecting the hydrologic impacts of climate change. Earth Interact. 17 (22), 1–19.
Logachev, N.A., 2003. History and geodynamics of the baikal rift. Russ. Geol. Geophys. 44 (5), 391–406.
Ma, X., Yasunari, T., Ohata, T., Natsagdorj, L., Davaa, G., Oyunbaatar, D., 2003. Hydrological regime analysis of the Selenge River basin, Mongolia. Hydrol. Process. 17, 2929–2945. http://dx.doi.org/10.1002/hyp.1442.
Magnuson, J.J., Robertson, D.M., Benson, B.J., Wynne, R.H., Livingstone, D.M., Arai, T., Assel, R.A., Barry, R.G., Card, V., Kuusisto, E., Granin, N.G., Prowse, T.D., Stewart, K.M., Vuglinski, V.S., 2000. Historical trends in lake and river ice cover in the Northern Hemisphere. Science 289 (5485), 1743–1746.
McClelland, J.W., Holmes, R.M., Peterson, B.J., Stieglitz, M., 2004. Increasing river discharge in the Eurasian Arctic: consideration of dams, permafrost thaw, and fires as potential agents of change. J. Geophys. Res. 109, D18102. http://dx.doi.org/10.1029/2004JD004583.
Michalak, A.M., Anderson, E.J., Beletsky, D., Boland, S., Bosch, N.S., Bridgeman, T.B., Chaffin, J.D., Cho, K., Confesor, R., Daloglu, I., Depinto, J.V., Evans, M.A., Fahnenstiel, G.L., He, L., Ho, J.C., Jenkins, L., Johengen, T.H., Kuo, K.C., Laporte, E., Liu, X., McWilliams, M.R., Moore, M.R., Posselt, D.J., Richards, R.P., Scavia, D., Steiner, A.L., Verhamme, E., Wright, D.M., Zagorski, M.A., 2013. Record-setting algal bloom in Lake Erie caused by agricultural and meteorological trends consistent with expected future conditions. Proc. Natl. Acad. Sci. USA 110 (16), 6448–6452.
Moore, M.V., Hampton, S.E., Izmest'eva, L.R., et al., 2009. Climate change and the World's "Sacred Sea"-Lake Baikal, Siberia. Bioscience 59 (5), 405–417.
Mun, Y., Ko, I.H., Janchivorj, L., Gomboev, B., Kang, S.I., Lee, C.H., 2008. Integrated Water Management Model on the Selenge River Basin – Statys Syrvey and Investigation (Phase I). Korea Environment Institute, Seoul.
Poulter et al., 2013. Recent trends in Inner Asian forest dynamics to temperature and precipitation indicate high sensitivity to climate change. Agric. For. Meteorol. 178–179, 31–45. http://dx.doi.org/10.1016/j.agrformet.2012.12.006.
Priess, J.A., Shweitzer, C., Wimmer, F., Batkhishig, O., Mimler, M., 2011. The consequences of land-use change and water demands in Central Mongolia. Land Use Policy 28, 4–10.C.
Serreze, M.C., Walsh, J.E., Chapin, F.S., Osterkamp, T., Dyurgerov, M., Romanovsky, V., Oechel, W.C., Morison, J., Zhang, T., Barry, G., 2000. Observational evidence of recent change in the northern high-latitude environment. Clim. Chang. 46, 159–207.
Sharkhuu. N., 2003. Recent changes in the permafrost of Mongolia. In: Permafrost, Phillips, M., Springman, S.M., Arenson, L.U. (Eds.), vols. 1–2, pp. 1029–1034.
Slater, A.G., Lawrence, D.M., 2013. Diagnosing present and future permafrost from climate models. J. Clim. 26 (15), 5608–5623. http://dx.doi.org/10.1175/JCLI-D-12-00341.1.
Smith, L.C., Pavelsky, T.M., MacDonald, G.M., Shiklomanov, A.I., Lammers, R.B., 2007. Rising minimum daily flows in northern Eurasian rivers: a growing influence of groundwater in the high-latitude hydrologic cycle. J. Geophys. Res. 112, G04S47.
Stevens, B., Bony, S., 2013. What are climate models missing? Science 340. http://dx.doi.org/10.1126/science.1237554.
Taylor, K.E., Stouffer, R.J., Meehl, G.A., 2012. An overview of CMIP5 and the experiment design. Bull. Am. Meteorol. Soc. 93, 485–498.
Teutschbein, C., Seibert, J., 2012. Bias correction of regional climate model simulations for hydrological climate-change impact studies: review and evaluation of different methods. J. Hydrol. 456–457, 12–29. http://dx.doi.org/10.1016/j.jhydrol.2012.05.052.
Thorslund, J., Jarsjö, J., Chalov, S.R., Belazerova, E.V., 2012. Gold mining impact on riverine heavy metal transport in a sparsely monitored region: the upper Lake Baikal Basin case. J. Environ. Monit. 14, 2780–2792.
Törnqvist, R., Jarsjö, J., 2012. Water savings through improved irrigation techniques: basin-scale quantification in semi-arid environments. Water Resour. Manage 26, 949–962.

Trenberth, K.E., Asrar, G.R., 2012. Challenges and opportunities in water cycle research: WCRP contributions. Surv. Geophys. http://dx.doi.org/10.1007/s10712-012-9214-y.

UNESCO, 1996. Convention concerning the protection of the world cultural and natural heritage: Report, 2-7/12/1996, Merida, Mexico. <http://whc.unesco.org/archive/repcom96.htm#754>.

Varis, O., Kajander, T., Lemmelä, R., 2004. Climate and water: from climate models to water management and vice versa. Climatic Change 66, 321–344.

Voropay, N.N., Maksyutova, E.V., Balybina, A.S., 2011. Contemporary climatic changes in the Predbaikalie region. Environ. Res. Lett. 6, 045209. http://dx.doi.org/10.1088/1748-9326/6/4/045209.

Wu, T., Wang, Q., Zhao, L., Batkhishig, O., Watanabe, M., 2011. Observed trends in surface freezing/thawing index over the period 1987–2005 in Mongolia. Cold Reg. Sci. Technol. 69, 105–111. http://dx.doi.org/10.1016/j.coldregions.2011.07.003.

Zhao, L., Wu, Q., Marchenko, S.S., Sharkhuu, N., 2010. Thermal state of permafrost and active layer in central Asia during the international polar year. Permafrost Periglac. Process. 21, 198–207.